Humanoid Vertical Jumping based on GRF and Inertial Forces Optimization

Sophie Sakka, Kazuhito Yokoi

Humanoid Vertical Jumping based on Force Feedback and Inertial Forces Optimization

Sophie Sakka and Kazuhito Yokoi
AIST/CNRS Joint Japanese-French Robotics Research Laboratory (JRL)
Intelligent Systems Research Institute (ISRI), AIST
Central 2, 1-1-1 Umezono, Tsukuba 305-8568, Japan
sophie.sakka@aist.go.jp

***Abstract*— This paper proposes adapting human jumping dynamics to humanoid robotic structures. Data obtained from human jumping phases and decomposition together with ground reaction forces (GRF) are used as model references. Moreover, bodies inertial forces are used as task constraints while optimizing energy to determine the humanoid robot posture and improve its jumping performances.**

***Index Terms*— Humanoid robotics, jumping pattern generation, inertia optimization.**

I. Introduction

The humanoid robotic concept appeared in the last 20 years. The Japanese institutions brought into the scene of the robotic research a considerable gap with the first apparition of the Honda humanoid robot in the 1997. Since then, many robotic research organisms, from all around the world, considered to built humanoid platforms and humanoid national program are launched in many countries (HRP, Robo-erectus, KHR [11], GuRoo, Dav, BH1 and many others) [3], [5], [14], [15].

A humanoid robot is a complex redundent robotic system having the particularity to be inspired from the human body structure kinematics, or even from human appearance in some cases. Humanoids have a large number of degrees of freedom (dof) and are usually modeled as tree structures grouping several open links chains.

The tendency in reducing their weight and their size may lead to a fragile mechanical structure and since the actuators are all together reduced in size they need reduction mechanism which generally cannot support high impact forces. Consequently it becomes challenging to design controllers able to mimic some of the human-like fast dynamics while meeting mechanical and actuators limitations.

Up-to-now, humanoids platforms have been designed for slow dynamics walking patterns. Consequently, experimental systems are limited in terms of locomotion diversity, namely the ones inducing fast dynamics. This is because of their technological design limitations. Fast dynamic gaits, for example running or jumping (or more precisely, jumping *for* running [17], [13], [9], are still actively under investigation and spectacular results have recently been produced with ASIMO running [6]. Dynamic equilibrium unbalance approaches for full body pattern motion definitions are still being formulated, even if some recent results for new mobility patterns tend to get closer to the robot dynamic balance stability limits [1][4] and therefore allow new mobility patterns.

In order to generate walking patterns for different locomotion kinematics, the common way of most existing approaches is to precompute reference trajectories. Subsequent controller design and gains setting are then performed to make things work experimentally as close as possible to the theoretical algorithms. Handling of dynamic balance stability is mostly made with autonomous independent modules. For simple walking patterns, in known environments, this way seems to work quite fine in many humanoid platforms and seems to be open to evolve to more complex patterns.

Similarly, using precomputed reference trajectory, this paper proposes a method for humanoid vertical jumping (i.e. leading to a humanoid takeoff from ground). The reference trajectory is derived from a thorough study of the way we, humans, jump. The humanoid reference jumping trajectory is designed to be as close as possible, under predefined constraints, to the human one which is derived from Ground Reaction Forces (GRF, and not from off line trajectory monitoring); this is presented in section 2. Human jumping phases decomposition and GRF data are used as references for pattern generation, this is presented in section 3. In section 4, how bodies' inertial forces can be optimized to determine the humanoid body posture in order to improve its jumping performances is discussed. These results are illustrated through a dynamic simulation of a humanoid vertical jump using OpenHRP integrated simulator with HRP-2 robot model.

II. Humanoid jumping representation

A. Procedure

The humanoid vertical jump model uses the human jump as a reference. There are many evident differences between the two "systems"; among them: foot bending capability, bodies mass repartition, joints and muscles quantity and characteristics, compliance, shock absorption capabilities. Therefore the human reference model provides the only external output of the human jump, i.e. the produced vertical acceleration of the center of mass (CoM) with the desired flight height. As we will see, we will make use of these data that are obtained by measuring the vertical component of the feet/ground reaction force together with the motion. Other parameters, such as the human joints

angle or joints speed values are not considered whereas other studies, such as in [2][7][16] considered these data on their developed mimetic approaches.

This paper focuses on the study of launching stage of the vertical jump, and more precisely defines a jumping function which groups jumping phase and takeoff impulse described thereafter. The launching stage of the jump is fundamental as it allows to meet the jump requirements (desired height, flight and landing stability) while minimizing robot actuators resources. This stage is divided in three successive phases:

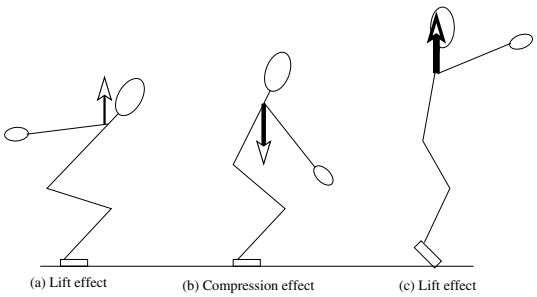

Fig. 1. Qualitative effects of arm-swing.

1) **Counter movement phase**: it mainly simulates the human muscular explosive[1] jumping movement. On robots, this phase can be associated to initial launching configuration. For humans, the way this phase is performed influences muscle conditions, consequently the performance of one's jump. This is not the case of humanoids since they are robotics systems and the actuator can produce max torques from any static configuration (i.e. in the contrary to muscles, they do not require a specific "warp-up" phase).
2) **Jumping phase**: The jumping phase denotes the propulsion phase of the jump. The body is subject to rising vertical acceleration until its speed reaches 86% of the takeoff desired speed for a medium jump. This proportion increases when the jump is required to reach more important heights, i.e. when one needs to get close to the maximal biological capabilities. Movement amplitude (feet/hip distance between the jumping initial configuration and the jumping extension configuration) and the value of vertical acceleration are the two key parameters that characterize the jumping phase.
3) **Takeoff impulse**: this phase lasts the shortest time; it is the most demanding in matter of system power resources. Takeoff impulse has two aims: the first one is to adapt precisely the actual body speed to the required takeoff speed in order to reach the desired jump height, the second one counterbalances the inertial effects created by the discontinuity of the GRF at the takeoff time. This allows to reduce brutal torque variation in the knees using a feet retraction procedure.

[1]All along the paper we are using the terminology adopted in the biomechanics field, we think that meaning can be guessed easily from the employed terms [18].

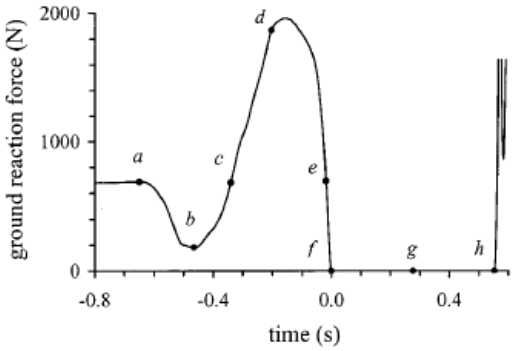

Fig. 2. Ground reaction force for a human maximal capacities vertical jump with counter-movement obtained using a force platform [12]

These three main phases are spotted on Fig. 2, which shows an experimental curve of the GRF for human maximal jump with counter-movement measured using a force platform [12]. The counter-movement is labeled from *a* to *c*, where the system is stabilized in jumping configuration (figure 1.a). The jumping phase is between *c* and *d* and the final impulse is around point *d*. The relation linking acceleration to reaction forces is given by the system of fundamental equations of motion before takeoff, that is:

$$\left\{ \begin{array}{c} m\ddot{\mathbf{X}}_G \\ \delta_{r/\Sigma} \end{array} \right\}_G = \left\{ \begin{array}{c} \mathbf{F}^{\text{ext}} \\ \mathbf{M}^{\text{ext}}_{G/\Sigma} \end{array} \right\}_G \quad (1)$$

where m denotes the total mass of the humanoid robot, $\ddot{\mathbf{X}}_G$ is the Cartesian acceleration vector of the system CoM G, $\delta_{r/\Sigma}(G)$ is the system resulting dynamic momentum in the reference frame noted Σ. $\mathbf{F}^{\text{ext}} = \sum \mathbf{F}^{\text{ext}}_i = \mathbf{R} + m\mathbf{g}$ and $\mathbf{M}^{\text{ext}}_{G/\Sigma} = \sum \mathbf{M}^{\text{ext}}_{G_i/\Sigma}$ are respectively the resulting external forces and momentum applied to the body and expressed at the CoM. $\mathbf{g} = -9.81\mathbf{x}^3_\Sigma$ [m.s^{-2}] denotes the gravity acceleration vector ($\mathbf{x}^3_\Sigma$ denotes the vertical component of the reference world frame Σ).

Considering Eq. 1, CoM acceleration and GRF values have the same profile of evolution with time. Then, acceleration of the CoM shows a linear profile through the whole jumping function (which includes jumping phase and takeoff impulse). The optimization of trajectories described in the following sections concentrates on the study of this particular function, but first we precise thereafter the influent parameters of the jump.

The parameters influencing the humanoid jump are illustrated on Fig. 3.

The jump (or flight) height denotes the desired jump requirements. It corresponds to the jumping target and is given by the user or the embedded planner. The jump target can be defined either from a hand reaching target or a feet height target according to the task. Our study focuses on the last situation (i.e. the desired feet height). The flight height is influenced by, see Fig. 3:

- the technological limitations (for exemple motors limits), which also define other important parameters such

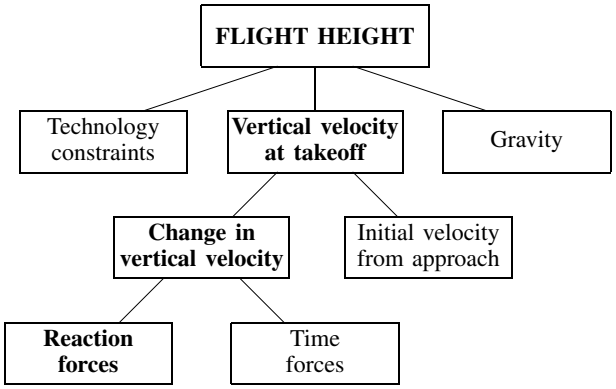

Fig. 3. Jumping performances influent factors

as the maximal reachable jump height,
- the vertical velocity at takeoff, and
- gravity which remains constant.

The only parameter that can be modified according to jumping requirements is the body vertical velocity at takeoff, which relies both on the approach initial velocity and on the instantaneous impulse changes. The approach initial velocity remains nil as humanoid jumps starts from a static standing configuration. Time forces describe external forces (external disturbance like trampolin reaction force) which are not considered in this study. Then only ground reaction forces can be modified for the system to match the jumping requirements.

B. Desired height of jump

We define the three position vectors as

- $\mathbf{X}_{\max}(t) = [X^1_{\max}, X^2_{\max}, X^3_{\max}]$ the absolute position of the system CoM in the reference frame;
- $\mathbf{X}(t) = [X^1, X^2, X^3]$ the relative position of the system CoM in the feet frame;
- $\mathbf{X}_d(t) = [X^1_d, X^2_d, X^3_d] = \mathbf{X}_{\max}(t) - \mathbf{X}(t)$ the absolute position of the feet in the reference frame.

The vertical components of these three vectors are schematized on Fig. 4. $x_{\max}$ represents the humanoid robot CoM maximal height, and x_d the maximal feet height, matching the desired height of the jump. During the aerial phase of

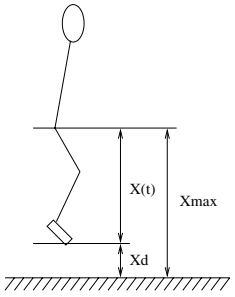

Fig. 4. Notations.

the jump, the robot may be considered as a projectile in free flight and is subject only to the gravity acceleration. The changes in kinetic energy and gravitational potential energy between the instant at takeoff and at maximal peak of the jump leads to the expression of the desired CoM speed at takeoff $\dot{X}_{\text{to}}$ according to the desired maximal peak $x_{\max}$:

$$\dot{X}^2_{\text{to}} = 2g(x_{\max} - X(t_{\text{to}})) \tag{2}$$

The CoM vertical trajectory, velocity and acceleration are then described by the traditional free flight rigid body motion equations. The takeoff speed is the humanoid body speed to be reached at the end of the jumping process. It allows to make the link between the influent parameters after and before takeoff, i.e. between the desired feet/ground flight height x_d and the matching required impulse reaction force R^d_{GRF}, under the hypothesis that joints velocities and accelerations remain null during the flight phase.

III. The jumping phase

A. CoM desired motion

The jumping function describes the vertical acceleration of the CoM. The left side of system (3) defines the movement constraints with

$$\begin{array}{rcl} m\ddot{X}^1_G & = & 0 \\ m\ddot{X}^2_G & = & 0 \\ m\ddot{X}^3_G & = & R^d_{\text{GRF}} + mg \\ \delta^1_{r/\Sigma}(G) & = & 0 \\ \delta^2_{r/\Sigma}(G) & = & 0 \\ \delta^3_{r/\Sigma}(G) & = & 0 \end{array} \tag{3}$$

where R^d_{GRF} is the desired feet/ground reaction force. According to the human model, R^d_{GRF} matches to a linear function of time during the impulsion movement (Fig. 2). Considering the boundary constraints $\dot{X}^3_G(t_0) = 0$, $\ddot{X}^3_G(t_0) = 0$, and $\dot{X}^3_G(t_{\text{to}}) = \dot{X}_{\text{to}}$, the CoM equations of motion are obtained by the successive integration of the acceleration projected on the vertical axis:

$$\begin{array}{rcl} \ddot{X}^3_G(t) & = & \frac{2\dot{X}_{\text{to}}}{t^2_{\text{to}}}\, t \\ \dot{X}^3_G(t) & = & \frac{\dot{X}_{\text{to}}}{t^2_{\text{to}}}\, t^2 \\ X^3_G(t) & = & X^3_G(t_0) + \frac{\dot{X}_{\text{to}}}{3t^2_{\text{to}}}\, t^3 \end{array} \tag{4}$$

where $X^3_G(t)$ is the desired feet/waist relative trajectory, $X^3_G(t_0)$ the initial feet/hip distance. The desired reaction force R^d_{GRF} is calculated according to the desired inertia to lift the robot up to a desired height X^3_d.

$$R^d_{\text{GRF}} = \frac{2m\dot{X}_{\text{to}}}{t^2_{\text{to}}}\, t - mg \tag{5}$$

B. Jumping constraints

The motion constraints can be divided in three groups of constraints: System, behavior and task constraints.

1) System constraints: These constraints are related to the studied system, they define it and insure that the requested movement is *feasible*. They group mechanics and electrics constraints such as joint boundaries, actuators speed/torque and sensors range values and characteristics, system model. They cannot be removed or modified or violated.

In this study the system is defined by HRP-2 humanoid robot [10], [8]. This humanoid platform is a 30 dof structure equipped with ankles and wrists force sensors, gyroscope and accelerometer sensors. The robot is modeled using Lagrange's representation for the optimization such as

$$M\ddot{q} + B(q.\dot{q}) + G(q) - f\dot{q} + \Gamma_s = \Gamma \tag{6}$$

with $f\dot{q}$ and Γ_s representing respectively viscous and static friction terms, Γ denotes the torques vector. The matrices M, B and G group the terms of inertia, centrifugal, Coriolis and gravity forces acting on the system. q, $\dot{q}$ and $\ddot{q}$ denotes respectively the trajectories, velocities and accelerations vectors in the operational space.

2) Behavior constraints: This group of constraints define general behavior constraints such as maintaining balance for vertical standing for humanoid systems. They are common to several kinds of movements (tasks), can be switched to perform other kind of tasks and can be violated while generating automatically "reflex" counterbalance movements. They insure that a motion declared as feasible by the system constraints is *admissible* for the considered behavior.

3) Task constraints: This set of constraints is specific to the desired task. In the case of vertical jumping, they impose vertical motion of the CoM (Eq. 4) and desired speed at takeoff (Eq. 2).

The physics, mechanics and electrics constraints mentioned previously allow to restrict the system motion possibilities for vertical jumping. However, the problem remains under-constrained and the determination of one motion solution is made using trajectory optimization described in the next section.

IV. Bodies inertial forces distribution

A. Trajectory definition

Each joint trajectory is approximate by a 5-order time polynomial

$$q_j(t) = \sum_{i=0}^{5} a_i^j t^i \tag{7}$$

where index j denotes the dof ($j = 1..7$ as the symmetry keeps the motion in the sagittal plane). a_i^j denotes the polynomial constant coefficients. Joint velocity and acceleration are obtained using polynomial derivation of trajectory. The coefficients a_i^j are functions of the trajectory boundary conditions $(t_f, q_j^{\text{init}}, q_j^{\text{fin}}, \dot{q}_j^{\text{init}}, \dot{q}_j^{\text{fin}}, \ddot{q}_j^{\text{init}}, \ddot{q}_j^{\text{fin}})$ to determine. Each joint trajectory is divided in two sub-trajectories matching the jumping phase and the takeoff phase described in section 2.A. Boundary conditions for the two phases are:

- Jumping phase: null initial velocity and acceleration, $(\dot{q}_j^{\text{init}})_{\text{jp}} = 0$, $(\ddot{q}_j^{\text{init}})_{\text{jp}} = 0$
- Takeoff phase: null final velocity and acceleration, $(\dot{q}_j^{\text{fin}})_{\text{to}} = 0$, $(\ddot{q}_j^{\text{fin}})_{\text{to}} = 0$
- Trajectory, velocity and acceleration continuity, $(q_j^{\text{fin}})_{\text{jp}} = (q_j^{\text{init}})_{\text{to}}$, $(\dot{q}_j^{\text{fin}})_{\text{jp}} = (\dot{q}_j^{\text{init}})_{\text{to}}$, $(\ddot{q}_j^{\text{fin}})_{\text{jp}} = (\ddot{q}_j^{\text{init}})_{\text{to}}$.

So the 7 unknown parameters reduces to 5 unknown parameters for each phase and for each joint.

B. Inertial forces

The forces acting at the CoM of a given link can be used for estimating the link contribution to the GRF which is simply the sum of the forces at the CoMs of the links. The acting forces during motion of the D-link chain representing the robot are:

$$\mathbf{F} = \sum_i \sum_j (\mathbf{F}_{ij}^n + \mathbf{F}_{ij}^t) + \mathbf{F}^{cor} \tag{8}$$

where $\mathbf{F}_{ij}^n$ and $\mathbf{F}_{ij}^t$ are respectively the centripetal and tangential forces applied to link j resulting from the movement of joint i, $\mathbf{F}^{cor}$ are the Coriolis forces. The expression of $\mathbf{F}_{ij}^n$ and $\mathbf{F}_{ij}^t$ are given by:

$$\begin{aligned} \mathbf{F}_{ij}^n &= m_j d_{ij} \dot{\alpha}_i^2 \mathbf{n}_{ij} \\ \mathbf{F}_{ij}^t &= m_j d_{ij} \ddot{\alpha}_i \mathbf{t}_{ij} \end{aligned} \tag{9}$$

with

$$\begin{bmatrix} n_{ij} & t_{ij} \end{bmatrix}^T = R_\Sigma^{ij} \begin{bmatrix} x_W & z_W \end{bmatrix}^T$$

where R_W^{ij} is the transformation matrix from the world frame noted Σ_W to the local frame Σ_{ij}. d_{ij} denotes the distance from joint i to the CoM of link j. A schematic

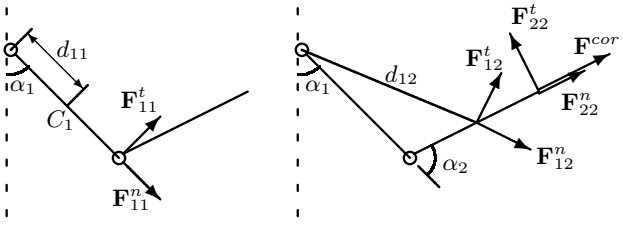

Fig. 5. Vector representation of inertial forces acting on a two-link chain.

representation of these forces is shown on Fig. 5, considering only the 2-link system of the arms. The energy needed by the system to produce the global inertial forces in the operational space is directly related to the desired speed at takeoff through the impulse-momentum theorem.

$$\int_{t_{\text{jc}}}^{t_{\text{to}}} \mathbf{F} dt = m\dot{\mathbf{X}}_{\text{to}} \tag{10}$$

where t_{jc} denotes the time at initial jumping configuration. The system of Eq. (10) define the optimization task constraints while the optimization criteria refers to the total energy consumed by the system to meet these constraints:

$$J = \int_{t_{\text{jc}}}^{t_{\text{to}}} \max\left(\sum_{j=1}^{D} \left(\frac{R_j}{k_{em}^2}\Gamma_j^2 + \Gamma_j \dot{q}_j\right), 0\right) \text{ dt} \tag{11}$$

where R_j and k_{em} denote j^{th} actuator characteristics, Γ_j the applied torque and $\dot{q}_j$ the operational speed.

C. Arm-swing contribution

Arm-swing motion while jumping is used to maximize the performances of the jump, i.e. to reach a greater height for a given impulsion or to distribute the joint torques such as reducing legs joints solicitations. Its qualitative effects are illustrated on Fig. 1; they result from the inertial forces caused by the rotation of the links of the arms. In this section we study the effects of fast movements of the arms alone. Inertial contribution of one arm according

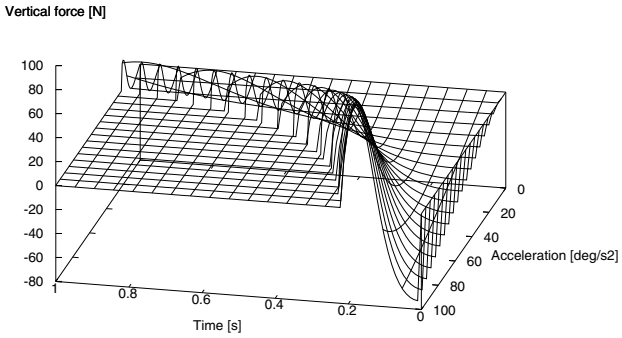

Fig. 6. Inertial forces resulting from the acceleration of the joint shoulder.

to shoulder acceleration can be observed on Fig. 6. The value of inertial contribution mostly relies on speed and acceleration values, but also on the movement amplitude.

For arm motion, optimization algorithm proposes a solution illustrated by Fig. 7. The two sub-trajectories divide the motion as follows (Fig. 9): the first one shows a wild circular motion leading to system CoM desired vertical ending velocity and acceleration. The second subtrajectory lasts very short time and consists in straitening the arm. The effect is maintaining vertical inertial forces created in the previous motion while suddenly dropping velocities to zero.

For the jumping phase, torques, energy consumption and evolution of CoM velocities are given on Fig. 8 and 9. They show the main use of the shoulder joint which allow to obtain maximal inertial effects by using the global weight of the arm. So the main part of vertical inertial effects comes from the motion of the shoulder. The elbow motion insures the vertical direction of resulting inertial effects until its ending. According to leg propulsion phase duration, arms optimal contribution to feet/ground reaction force is up to 100N, which represents 12.5% of a vertical 800N total vertical propulsion force.

The optimization results for full body jumping motion are shown on snapshots of OpenHRP simulation (Fig. 10). Figure 10.a shows the initial configuration of the system while 10.b, 10.c and 10.d illustrate respectively initial, intermediate and final configurations of the optimized jumping function. The arm motion is counter-balanced with mainly bending of the trunc in order to keep the robot CoM trajectory vertical.

Figure 10 also illustrates the bending of the upper

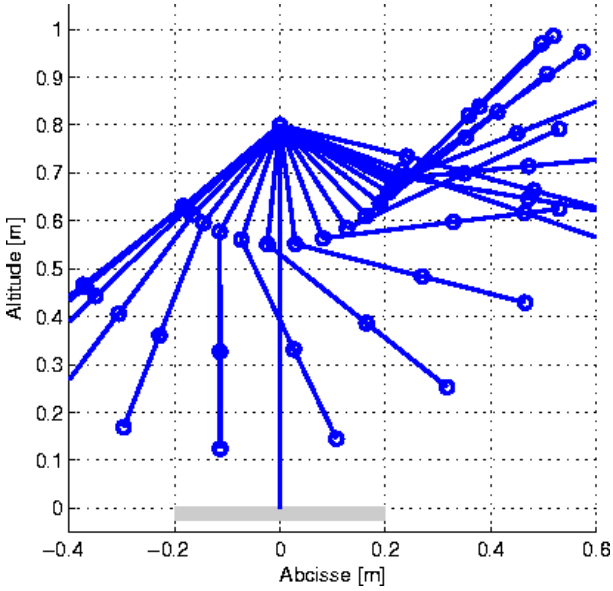

Fig. 7. Schematic representation of the two sub-trajectories for arms motion.

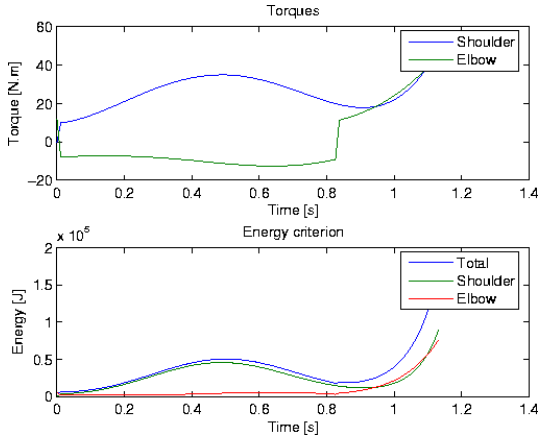

Fig. 8. Arms torques and energy values.

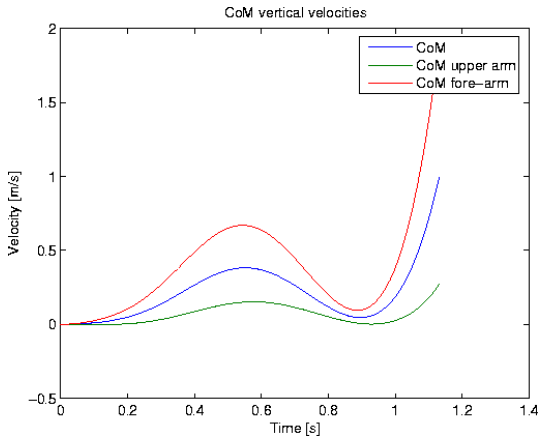

Fig. 9. Bodies center of mass velocities.

part of the body, where arm-swing and legs, the main propulsion actors, are combined for the jump. Differences in configurations can be distinctly observed on the Fig. 10

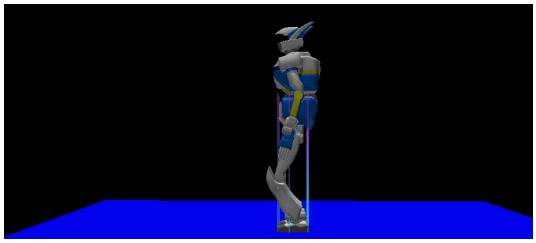

(a) Initial configuration

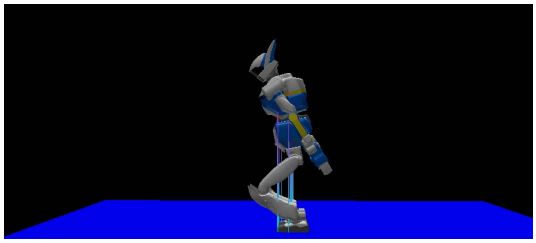

(b) Counter movement configuration

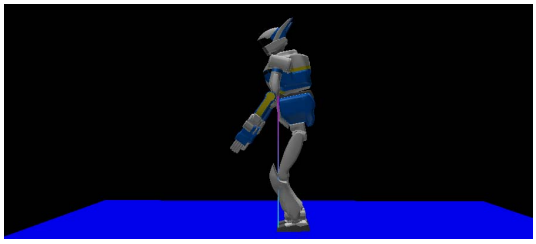

(c) Jumping function

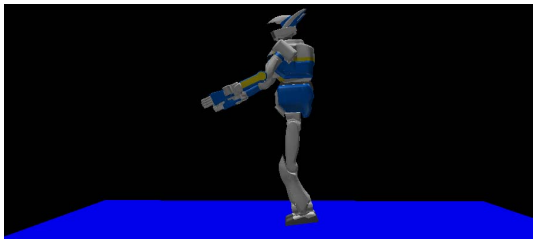

(d) Aerial phase

Fig. 10. Jump snapshots extracted from OpenHRP simulation.

because jump height requirements were chosen high for a demonstration purpose. The trunk bending is not so obvious for smaller jumps, such as for the 800N reaction force jump example, previously mentioned.

V. Conclusion

This paper presents an approach based on feet/ground reaction forces to make humanoid perform vertical jumps. The reaction forces remain constant during the jumping phase and directly depend on the desired flight height and the robot parameters.

Humanoid body motion was determined using maximal vertical inertial forces distributed on all the individual bodies in order to improve the performances of the jump, i.e. to be able to perform higher jump with similar legs impulse or similar jump performances with less legs actuators solicitations.

The quantification of robot jump performances according to maximal reached height accessible and actuators total and local solicitations is the next step of the study. Establishment of such jumping quality criteria can be used for any kind of robot and help to compare objectively different approaches -or different robots- performances.

Then, the modeling of damping procedure for landing, minimizing the impact forces when ground landing, remains the main objective as perspective.

Acknowledgment

This research is supported by a post-doctoral Fellowship of Japan Society of Promotion for Science (JSPS), and by a Research Grant of JSPS.

References

[1] K. Arikawa and T. Mita, "Design of Multi-DOF Jumping Robot", Proc. of Int. conf. on Robotics & Automation (ICRA), pp. 3992-3997, 2002.

[2] O. Bruneau, F.B. Ouezdou and J.-G. Fontaine, "Dynamic Walk of a Bipedal Robot Having Flexible Feet", Proc. of the 2001 IROS, 2001.

[3] M. Gienger, et al., "Toward the Design of a Biped Jogging Robot", Proc. of Int. conf. on Robotics & Automation (ICRA), pp. 4140-4145, 2001.

[4] Y. Guan, K. Yokoi, N.E. Sian and K. Tanie, "Feasibility of Humanoid Robots Stepping Over Obstacles", Proc. of the 2004 IROS, 2004.

[5] K. Hirai, M. Hirose, Y. Haikawa and T. Takenaka, "The Development of Honda Humanoid Robot", Proc. of Int. conf. on Robotics & Automation (ICRA), pp. 1321-1326, 1998.

[6] http://world.honda.com/HDTV/ASIMO/

[7] A.J. Ijspeert, J. Nakanishi and S. Schaal, "Movement Imitation with non linear Dynamical Systems in Humanoid Robots", Proc. of Int. conf. on Robotics & Automation (ICRA), pp. 1398-1403, 2002.

[8] S. Kajita, F. Kanehiro, K. Kaneko, K. Fujiwara, K. Harada, K. Yokoi and H. Hirukawa, "Resolved Momentum Control: Humanoid Motion Planning based on the Linear and Angular Momentum", Proc. of the 2003 IROS, pp. 1644-1650, 2003.

[9] S. Kajita, T. Nagasaki, K. Kaneko, K. Yokoi and K. Tanie, "A Hop towards Running Humanoid Biped", Proc. of Int. conf. on Robotics & Automation (ICRA), pp. 629-635, 2004.

[10] K. Kaneko, F. Kanehiro, S. Kajita, H. Hirukawa, T. Kawasaki, M. Hirata, K. Akachi and T. Isozumi, "Humanoid Robot HRP-2", Proc. of Int. conf. on Robotics & Automation (ICRA), 2004.

[11] J.H. Kim and J.H. Oh, "Walking Control of the Humanoid Platform KHR-1 based on torque Feedback Control", Proc. of Int. conf. on Robotics & Automation (ICRA), pp. 623-629, 2004.

[12] N.P. Linthorne, "Analysis of standing vertical jumps using a force platform", Am. J. Phys. **69**(11), pp. 1198-1204, 2001.

[13] K. Nagasaka, Y. Kuroki, S. Suzuki, Y. Itoh, J. Yamaguchi, "Integrated Motion Control for Walking, Jumping and Running on Small Bipedal Entertainment Robot", Proc. of Int. conf. on Robotics & Automation (ICRA), pp. 3189-3194, 2004.

[14] K. Nishiwaki, T. Sugihara, S. Kagami, F. Kanehiro, M. Inaba and H. Inoue, "Design and development of Research Platform for Perception-Action Integration in Humanoid Robot: H6", Proc. of the 2000 IROS, pp. 1559-1564, 2000.

[15] Y. Ogura, H. Aikawa, H. Lim and A. Takanishi, "Development of a Human-like Walking Robot", Proc. of Int. conf. on Robotics & Automation (ICRA), pp. 134-140, 2004.

[16] N.S. Pollard, J.K. Hodgins, M.J. Riley and C.G. Atkeson, "Adapting Human Motion for the Control of a Humanoid Robot", Proc. of Int. conf. on Robotics & Automation (ICRA), pp. 1390-1397, 2002.

[17] M.H. Raibert, Jr H.B. Brown and M. Chepponis, "Experiments in Balance with a 3D One-Legged Hopping Machine", International Journal of Robotics Research, **3**(2), pp 75-92, 1984.

[18] V.M. Zatsiorsky, "Kinetics of Human Motion", Human Kinetics ed., The Pennsylvania State University, 2002.